

ARTICLES

S₂ and S₁ States Deactivation of Thiocoumarin in *n*-Hexane and Acetonitrile Studied by Femtosecond Fluorescence Upconversion and Transient Absorption SpectroscopiesGotard Burdzinski,^{*,†} Marcin Ziolk,[‡] Jerzy Karolczak,^{†,§} and Andrzej Maciejewski^{†,§}

Quantum Electronics Laboratory, Faculty of Physics, Adam Mickiewicz University, Umultowska 85, 61-614 Poznan, Poland, Center for Ultrafast Laser Spectroscopy, Adam Mickiewicz University, Umultowska 85, 61-614 Poznan, Poland, and Photochemistry Laboratory, Faculty of Chemistry, Adam Mickiewicz University, Grunwaldzka 6, 60-780 Poznan, Poland

Received: June 17, 2004; In Final Form: September 14, 2004

We have studied the unusual photophysics of a thioketone, thiocoumarin, in *n*-hexane and in acetonitrile by femtosecond fluorescence up-conversion and transient absorption spectroscopies. The lifetime of the S₂ state is found to be as short as 450 ± 50 fs in *n*-hexane and 130 ± 50 fs in acetonitrile, whereas the S₁ lifetime is about 10 ps. We propose that the fast S₂-state deactivation is governed by a conical intersection point linking the S₂ with S₁ potential energy surfaces. Direct absorption from the S₁ state of thioketones has been observed for the first time.

Introduction

Aromatic thioketones show many interesting spectral and photophysical properties including direct S₀→T₁ absorption, thermally activated S₁-fluorescence, well-resolved S₀→S₁, S₀→S₂, and S₀→S₃ absorption bands, fluorescence from the S₂ state, and phosphorescence from the T₁ state in solution at room temperature.^{1–4} In perfluorohydrocarbons, the S₂ (π,π*) state decay is exclusively intramolecular due to the weak solute–solvent interaction. The long S₂ state lifetime (τ_{S2} > 10⁻¹⁰ s), due to a large ΔE(S₂ – S₁) energy gap, and a high radiative rate constant (k_{S2→S0} ~ 10⁸ s⁻¹) is responsible for an unusual fluorescence from the S₂ state. This long S₂ state lifetime contrasts with the insignificant emission observed from the S₁ (n,π*) state due to a low radiative rate constant (k_{S1→S0} ~ 10⁵ s⁻¹) and an ultrafast intersystem crossing to the T₁ state (usually τ_{S1} ~ 5 × 10⁻¹³ s).⁵ In all other solvents except perfluorohydrocarbons, irrespective of polarity and protic character, the S₂ state is known to be extremely short-lived because of an efficient intermolecular quenching^{1,3,4,6–9} or intracomplex deactivation as in the hydrogen-bonded thioketone–water complex.¹⁰

In this paper, we present the properties of thiocoumarin (TC), which exhibits behavior atypical of other thioketones. First, our study has revealed that the S₂ state lifetime is extremely short (τ_{S2} < 500 fs) in *n*-hexane and in acetonitrile, which cannot be explained by high reactivity toward the solvent molecules. It means that the S₂ state deactivation is an intramolecular process, which can be rationalized by the occurrence of a possible conical intersection point linking S₂ with S₁. As a consequence, the S₂ state lifetime, τ_{S2}, is shorter than that of the S₁ state, τ_{S1} ≈ 10

ps, in contrast to the usual thioketone behavior: τ_{S2} > τ_{S1}. The S₁ state of TC is long-lived compared to those of the other thioketones due to the large energy gap ΔE(S₁ – T₁) which reduces the rate of the intersystem crossing process leading the S₁(n,π*) state to the T₁(π,π*) state. We have performed femtosecond transient absorption experiments to characterize the species formed upon the S₂ state deactivation. Direct absorption from the S₁ state has been reported for the first time for thioketones. To obtain direct kinetic information on the S₂ population, we have also applied the femtosecond fluorescence up-conversion technique.

Experimental Section

Femtosecond fluorescence up-conversion measurements were performed in a 1 mm thick cell moving in a plane perpendicular to the excitation beam in order to minimize sample heating. To rule out the influence of photochemical decomposition, the sample was renewed after every single scan. The thioketone concentration was approximately 1 × 10⁻³ M. The details of the experimental setup have been described previously.^{11,12} The pump wavelength was set at 380 nm. An instrument response function of 340 fs (fwhm) was obtained by mixing the residual excitation pulse with the gate pulse. The simplex method was used as the fitting procedure; after deconvolution, the time resolution was about 100 fs.

For the femtosecond transient absorption measurements, we used the setup also described in detail earlier.¹³ The output of the laser system (femtosecond titanium-sapphire) was set at 1 kHz repetition rate providing pulses of about 100 fs duration. The probe beam passed through an optical delay line consisting of a retroreflector mounted on a computer-controlled motorized translation stage and then converted to white light continuum (in 2 mm rotating calcium fluoride plate), whose diameter was 2–5 times smaller than that of the pumping beam. A grating

* Corresponding author. Fax: +48-61-829-5155. E-mail: gotardb@amu.edu.pl.

† Quantum Electronics Laboratory, Faculty of Physics.

‡ Center for Ultrafast Laser Spectroscopy.

§ Photochemistry Laboratory, Faculty of Chemistry.

polychromator was used in conjunction with a thermoelectrically cooled CCD camera to record the spectra. To improve the signal-to-noise ratio, the transient absorption measurements were performed in the two-beam geometry (probe and reference) with two synchronized choppers in the pump and probe paths, respectively, which allowed substantial elimination of the influence of the laser beam fluctuations and, consequently, measurements of much lower values of the optical density changes. With this experimental setup, absorbance changes (ΔA) can be measured with an accuracy of ± 0.0005 in the 300 to 700 nm spectral range. The thickness of the flowing sample was 2 mm. The pulse energy for the 400 nm pump wavelength was 20 μJ . All of the spectra analyzed were corrected for group velocity dispersion effect (GVD) according to the numerical scheme presented in ref 14. A signal with the correct time delay was determined by linear interpolation between two signals at the closest time delays taking into account the chirp of the white light continuum. The chirp (about 790 fs in the analyzed spectral range 330–600 nm) was obtained by measuring two-photon absorption in a very thin (150 μm) BK7 glass plate. An additional contribution to the chirp (about 290 fs in the spectral range 330–600 nm), due to the front window of the 1 mm thick fused silica sample cell, was calculated from the Sellmeier equation. The transient absorption signals originating from the pure solvent were subtracted from the data collected.¹⁵ All our fits of the kinetic curves involved the temporal instrumental function, taking into regard the cell thickness and hence the dispersion of the delay between the pump and the probe (originating from different group velocities of pump and probe pulses in the sample).¹⁶ The real instrumental function $S(t)$ used for the convolution with the kinetic exponential functions was determined separately for each wavelength, with the help of the following formula:¹⁶

$$S(t) = S_0 \exp\left(-\frac{2.3A}{\tau_{\text{GDD}}t}\right) \left[\text{erf}\left(\frac{t}{\tau} - \frac{2.3A}{\tau_{\text{GDD}}}\right) - \text{erf}\left(\frac{t}{\tau} - \frac{2.3A}{\tau_{\text{GDD}}}\frac{\tau}{2} - \frac{\tau_{\text{GDD}}}{\tau}\right) \right]$$

where S_0 is the amplitude, A denotes the sample absorbance at the excitation wavelength, and τ_{GDD} expresses the difference between transit times of the pump and probe pulses through the sample (calculated from the Sellmeier equation for given solvent, sample thickness, pump and probe wavelengths). The term τ denotes the temporal duration of the pump–probe cross correlation function unaffected by dispersion and was determined from the two-photon absorption in BK7 (excitation 400 nm). The two-photon absorption fwhm is $\tau_{\text{fwhm}} = 150$ fs, giving $\tau = 108$ fs ($\tau = 0.72 \tau_{\text{fwhm}}$). For example, broadening of more than 10% of the initial temporal width occurs when $\tau_{\text{GDD}}/\tau_{\text{fwhm}} > 0.6$, which in the case of our experimental conditions means that probe wavelength is shorter than 365 nm or longer than 445 nm for *n*-hexane.

All measurements were performed at room temperature (20 °C). TC was synthesized and purified by the methods described elsewhere.¹⁷ Acetonitrile (anhydrous, Aldrich) and *n*-hexane (for fluorescence, Merck) were used as received. The molecular rotational diffusion effects were eliminated by using the magic-angle configuration in all experiments.

Results

First, we recall steady-state absorption and emission results which are very similar in various solvents (*n*-hexane, benzene,

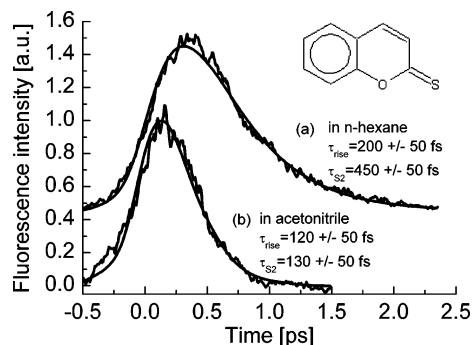


Figure 1. Normalized experimental decays of fluorescence at 490 nm obtained upon 380 nm photoexcitation of TC (1×10^{-3} M) in (a) *n*-hexane and (b) acetonitrile. The best fits using a convolution function of the instrument response with biexponential decay kinetics and the corresponding lifetimes τ_{S_2} and rise time τ_{rise} are also given. The kinetic profiles are vertically shifted for better presentation. The “time zero” corresponds to the peak of the instrument response function. The structural formula of a TC molecule is shown as inset.

methanol, and perfluorohydrocarbons).¹⁷ No aggregation of TC molecules has been detected by steady-state absorption for the concentration varied from 10^{-6} to 10^{-3} M. The $S_0 \rightarrow S_2$ absorption band is located in the 320–435 nm spectral range, peaking at 370 nm ($\epsilon \sim 11\,000 \text{ mol}^{-1} \text{ dm}^3 \text{ cm}^{-1}$) and is spectrally well resolved from that of the $S_0 \rightarrow S_3$ transition. The energy gap $\Delta E(S_2 - S_1) \sim 6000 \text{ cm}^{-1}$ has been estimated from $S_0 \rightarrow S_1(n, \pi^*)$ absorption data and $S_2(\pi, \pi^*) \rightarrow S_0$ emission data, and this value is small relative to other thioketones. The $S_2 \rightarrow S_0$ emission band is located in the 420–580 nm range, and its spectral position is very sensitive to the excess of energy carried to the S_2 state upon photoexcitation $S_0 \rightarrow S_2$.¹⁷ A blue spectral shift and broadening of the emission band was observed when the excess increases, which indicates that the fluorescence originates from both relaxed and excited vibrational levels.¹⁷ The quantum yield of fluorescence is 6.5×10^{-5} in perfluorohydrocarbons and 5×10^{-5} in *n*-hexane, the same within the experimental error (30%). The quantum yield of triplet formation upon S_2 excitation is nearly 1.^{18,19} From PM3 CI calculations, the obtained values of spin–orbit coupling constants between the S_1 and T_1 states ($\sim 24 \text{ cm}^{-1}$) and S_2 and T_2 states ($\sim 20 \text{ cm}^{-1}$) are very high, whereas the value determined for the S_2 and T_3 states (0.018 cm^{-1}) is very low.¹⁷ The lowest triplet state T_1 of TC has been described by the (π, π^*) electronic configuration. For TC, a wide energy gap $\Delta E(S_1 - T_1) \sim 4000 \text{ cm}^{-1}$ and large Stokes shift (between steady-state absorption and emission bands) compared to other thioketones (benzopyranthione, xanthione) has been observed. A significant Stokes shift has been rationalized by a distortion of the TC structure upon the transition to the S_2 state.¹⁷

All of the hitherto attempts to observe S_2 absorption or fluorescence decay have been unsuccessful because of insufficient time-resolution of the apparatus used. The lifetime $\tau_{S_2} = 1$ ps was estimated from the Strickler–Berg equation and fluorescence quantum yield.¹⁷ Thus, we have attempted to determine τ_{S_2} in *n*-hexane and in acetonitrile by means of the femtosecond fluorescence up-conversion technique. To obtain a good signal-to-noise ratio, the pump wavelength was tuned to 380 nm in strong resonance with the $S_0 \rightarrow S_2$ transition. Figure 1 presents the results of fluorescence measurements performed for solutions of TC (1×10^{-3} M) in *n*-hexane and in acetonitrile. The fitting analysis was carried out using the biexponential function, $F(t) = A_1 \exp(-t/\tau_{S_2}) + A_2 \exp(-t/\tau_{\text{rise}}) + y_0$, where τ_{rise} is the rise time constant, $A_1 > 0$ and $A_2 < 0$ are amplitudes, and y_0 is a constant for fitting purposes. A convolution function

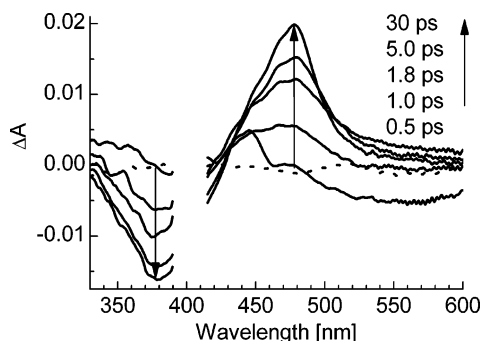


Figure 2. Transient absorption spectra recorded from -0.5 ps to 30 ps after photoexcitation of TC (1×10^{-3} M) in *n*-hexane at 400 nm. The spectrum at -0.5 ps (dotted line, the probe pulse is set 0.5 ps before the pump pulse) is also given to show the background signal. The spectral range 390–415 nm is not shown because it is disturbed by the scattered pumping beam (400 nm).

$\text{IRF}(t) \otimes F(t)$ was used to take into account the instrument response function $\text{IRF}(t)$. For all of the analyzed fluorescence wavelengths (from 430 to 540 nm), S_2 -state lifetime values of 450 ± 50 fs and 130 ± 50 fs were found in *n*-hexane and acetonitrile, respectively. In both solvents, the rise component τ_{rise} was about 150 fs. Such a rise component was not detected in the transient absorption kinetics (described below) recorded using a longer excitation wavelength (400 nm). We propose that the rise component observed in fluorescence up-conversion experiments results from excitation to the S_2 state with higher excess energy (3300 versus 2000 cm^{-1} in transient absorption experiments). As a consequence, the process of energy dissipation from Franck–Condon active modes (photoexcitation) looks different and can influence the build-up of fluorescence which, as we mentioned above, can occur from both nonrelaxed and relaxed vibrational levels. We attribute this rise time to intramolecular vibrational redistribution (IVR) in the S_2 state.²⁰

Femtosecond transient absorption measurements were recorded within a time window from -0.5 ps to 1 ns following 400 nm excitation of TC in *n*-hexane and acetonitrile. The spectral evolution and the kinetics are nearly the same in both solvents. Figure 2 shows the data obtained in the 330–600 nm spectral range upon 400 nm excitation of TC in *n*-hexane in the time range between -0.5 and 30 ps. No further spectral evolution in the 30–1000 ps time range is observed. At 0.5 ps the spectrum shows a negative band peaking at 550 nm and a positive one maximizing around 440 nm. Since sample photoexcitation leads TC directly to the S_2 state, the appearance of both bands results from a competition between the $S_2 \rightarrow S_0$ stimulated emission (predominant at 550 nm) and the S_2 absorption (predominant at 440 nm). In the 330–390 nm there is a competition between the ground-state depletion and the S_2 absorption. At a delay time of 1.8 ps the spectrum is different: a strong positive band arises at 470 nm with a broad tail extending to 600 nm, while the negative band maximizes at 370 nm. The first band is attributed to the S_1 absorption, while the negative one is dominated by the ground-state depletion. Note, that at 1.8 ps both the S_2 and T_1 states are almost unpopulated since the lifetime values τ_{S_2} and τ_{S_1} are 450 ± 50 fs and 9 ± 1 ps, respectively. At longer delay times, up to 30 ps, we still observe spectral changes: the positive band in the 450–490 nm range increases while the transient absorption signal in the 500–600 nm range decreases, and the ground-state depletion band reaches a maximal negative amplitude at 380 nm. Similar changes are observed in acetonitrile except that in the 500–600 nm range the spectrum is nearly constant for delay times longer than 1.3 ps. At 30 ps, the final absorption

spectrum can be attributed to the TC triplet state transition, with good agreement with the T_1 state spectrum recorded by nanosecond transient absorption.¹⁹

Figure 3 presents the transient absorption kinetic traces of TC in *n*-hexane and acetonitrile fitted with biexponential functions. The fitted time constants and amplitudes are given in Table 1. For TC in *n*-hexane, in the 370–390 nm spectral range, we observe the decay of the S_2 absorption signal with 590 ± 100 fs (in satisfactory agreement with 450 ± 50 fs value measured by fluorescence up-conversion technique) and decay of the S_1 absorption with 9.0 ± 1.0 ps time constant. Note that these decays are due to the existence of the S_2 and S_1 absorption bands at the spectral range of the ground-state depletion band which explains the negative transient absorption signals. The fitted offset parameter $y_0 = -0.0162$ corresponds mainly to the ground-state depletion amplitude. In 470–490 nm range, two rising kinetics are present, 780 ± 100 fs corresponds to the growth of the S_1 population (in this spectral region the signal from the S_2 -stimulated emission decay is compensated by the S_2 absorption), whereas 8.8 ± 1.9 ps can be attributed to the T_1 population rise. The longer S_1 rise time of 780 ± 100 fs compared to the S_2 decay time of 450 ± 50 fs can be explained by IVR in the hot S_1 state.

Finally, in the range 530–550 nm, the first value of 580 ± 100 fs results from the S_2 stimulated emission signal decay and the growth of S_1 population, whereas the second time constant of 11.4 ± 1.1 ps corresponds to the decay of the S_1 population. In acetonitrile, the time constants characterizing the S_2 and S_1 states are 180 ± 50 fs and about 9 ps respectively, the attribution of the characteristic spectra is the same, with the only difference being in the 530–550 nm range, where the decay of the S_1 absorption signal is overlapped by the rise in the T_1 absorption. We performed also preliminary measurements for TC in perfluorohydrocarbons. Since the signal was very noisy due to low solubility of TC in these solvents, we could only find out that the S_2 population decay and S_1 population rise occur with time constants shorter than 1 ps.

Discussion

The S_2 state lifetime of TC is extremely short in *n*-hexane (450 ± 50 fs) and acetonitrile (130 ± 50 fs), which cannot be explained by a high reactivity toward the solvent molecules, since in inert solvents (as perfluorohydrocarbons) the τ_{S_2} value is also short (< 1 ps) and the quantum yield of fluorescence is similar in all solvents. The intramolecular radiationless deactivation path of the S_2 state in thioketones leads to the S_1 state which has been well established.^{4,9,21} Note that the deactivation of the S_2 of TC to the T_3 state, lying a few hundred cm^{-1} below S_2 , can be excluded, since the spin–orbit coupling between these states is weak (0.018 cm^{-1}).¹⁷ Taking into account that only internal conversion is responsible for the S_2 deactivation, according to the energy gap law for the $\Delta E(S_2 - S_1) \sim 6000$ cm^{-1} , the S_2 state lifetime should be much longer: about 20 ps.¹⁷ That means that an additional intramolecular mechanism is responsible for very fast S_2 state deactivation. The most likely mechanism is the existence of a conical intersection point linking the S_2 state with the S_1 state. Note that the $\Delta E(S_2 - S_1)$ is small compared to that in the other thioketones and a distortion of the TC structure upon transition to the S_2 state can be expected. The latter is indicated by a large Stokes shift (between the steady-state absorption and emission bands) relative to that for the other thioketones (benzopyranthione, xanthione).¹⁷ A slightly smaller $\Delta E(S_2 - S_1)$ value for thioketones in acetonitrile than in *n*-hexane^{4,21} may explain the difference between τ_{S_2} values

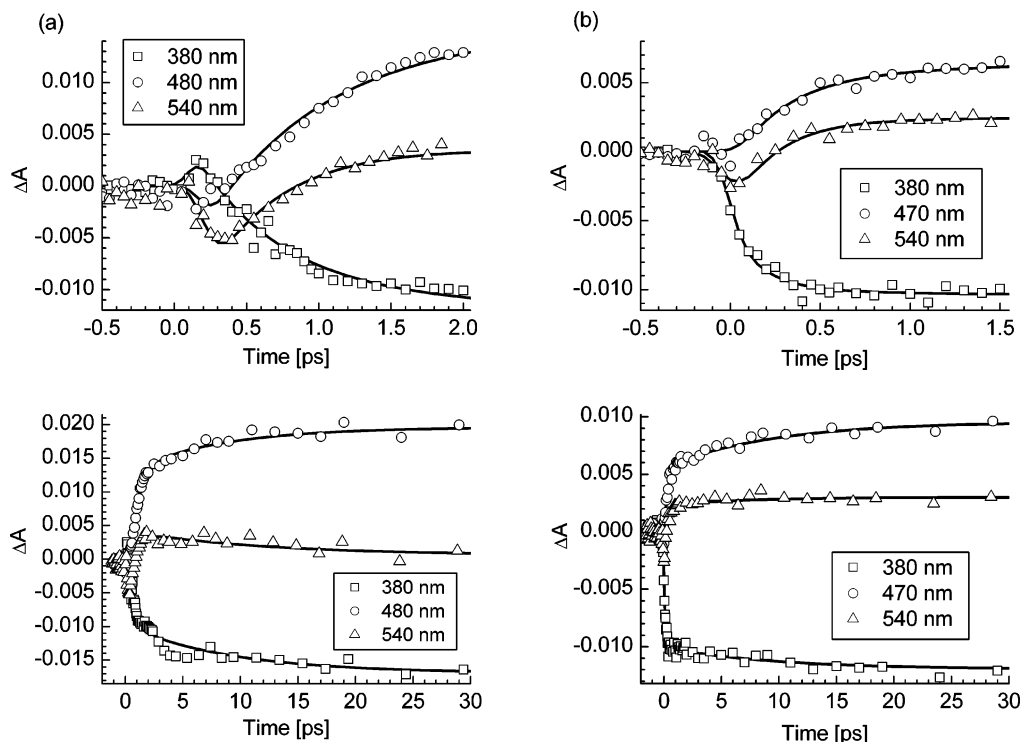


Figure 3. Time-dependence of the transient absorption signal at selected wavelengths in shorter (top) and extended (bottom) time ranges for TC in *n*-hexane (a) and in acetonitrile (b).

TABLE 1: Results of the Fitting Procedure of Transient Absorption Kinetic Traces for TC in *n*-Hexane (a) and in Acetonitrile (b)^a

spectral range	A_1	τ_1 [fs]	A_2	τ_2 [ps]	y_0
(a)					
470–485 nm	-0.0134	780 ± 100	-0.0057	8.8 ± 1.9	0.0191
370–390 nm	0.0110	590 ± 100	0.0066	9.0 ± 1.0	-0.0162
530–550 nm	-0.0095	580 ± 100	0.0036	11.4 ± 1.1	0.0008
(b)					
470–490 nm	-0.0056	300 ± 50	-0.0036	8.7 ± 1.0	0.0100
370–390 nm	0.0035	180 ± 50	0.0019	9.6 ± 1.0	-0.0117
530–550 nm	-0.0040	260 ± 50	-0.0007	7.8 ± 4.3	0.0030

^a The convolution of instrumental function with biexponential function $f(t) = A_1 \exp(-t/\tau_1) + A_2 \exp(-t/\tau_2) + y_0$ was fitted to the experimental data. The values of parameters and their errors were obtained by averaging the results of the fits performed every 5 nm in the given spectral range. Error of amplitudes: ± 0.0005 .

of TC in these solvents, because the position of the potential energy surfaces S_2 and S_1 can be influenced by solute–solvent interactions. The measured S_2 state lifetime of TC in *n*-hexane is also in good agreement with the lifetime (1 ps in perfluorohydrocarbons) estimated in ref 17 keeping in mind the similar quantum yields of fluorescence in *n*-hexane and perfluorohydrocarbons and assuming a similar value of the radiative rate constant in both solvents.

The S_1 state lifetime of TC in *n*-hexane and in acetonitrile is about 10 ps. The reactivity of TC in the S_1 state toward the solvent can be excluded, since its energy value is small. Efficient intersystem crossing leading the $S_1(n, \pi^*)$ to $T_1(\pi, \pi^*)$ is likely to be responsible for radiationless S_1 deactivation. It is accounted for by the strong spin–orbit coupling value ($\sim 24 \text{ cm}^{-1}$),¹⁷ the presence of the thiocarbonyl sulfur atom (heavy-atom effect), and the $^1(n, \pi^*) \rightarrow ^3(\pi, \pi^*)$ nature of the transition. Such a transition, according to the El-Sayed's rule, takes place much more efficiently relative to the $^1(n, \pi^*) \rightarrow ^3(n, \pi^*)$ transition.^{22,23} However, the τ_{S_1} value is much longer than the value experimentally determined for thioxanthone (~ 0.5 ps) and that

estimated for benzopyranthione (~ 0.5 ps) in fluid solution at room temperature.^{5,10} This might be explained by the fact that for TC the rate of the intersystem crossing process is reduced due to a larger energy gap between $^1(n, \pi^*)$ and $^3(\pi, \pi^*)$ states ($\sim 4000 \text{ cm}^{-1}$) than that for thioxanthone and benzopyranthione ($\sim 1000 \text{ cm}^{-1}$). Since the triplet T_1 state energy is lower than that of the S_1 state, the back transition to the S_1 state at room temperature can be excluded.

To summarize, the temporal evolution of transient absorption spectra of TC occurs according to the scheme $S_2 \rightarrow S_1 \rightarrow T_1$, in agreement with the T_1 formation efficiency, which is near to 100%.^{18,19} The lifetime of the S_2 state is much shorter than that of the S_1 state, which is typical of polyatomic aromatic molecules, but unusual for thioketones. At 1.8 ps time delay, the relative concentrations of the population in excited states of TC are about 5% in S_2 , 85% in S_1 , and 10% in T_1 for the τ_{S_2} and τ_{S_1} lifetime values in *n*-hexane. Thus, the transient absorption spectrum at this time delay (see Figure 2) corresponds mainly to the S_1 state, whose absorption spectrum, to our knowledge, has been reported for the first time for thioketones. The maximal absorption extinction coefficient for the S_1 state at 470 nm can be estimated as $\geq 6000 \text{ M}^{-1} \text{ cm}^{-1}$, taking into account $\geq 14\,000 \text{ M}^{-1} \text{ cm}^{-1}$ value for the T_1 in *n*-hexane (from other studies¹⁹).

Acknowledgment. The authors are grateful to Professor Max Glasbeek for the opportunity to perform the fluorescence up-conversion measurements at the Laboratory for Physical Chemistry at University of Amsterdam. The transient absorption measurements were performed at the Center for Ultrafast Laser Spectroscopy, Adam Mickiewicz University, Poznan, Poland. We are also grateful to Dr. G. Buntinx and Dr. O. Poizat, LASIR, Université de Lille I, Villeneuve d'Ascq, France, for the preliminary transient absorption studies. The paper was prepared under the financial support of KBN (Polish State Committee for Scientific Research) Grant No. 4T09A 166 24.

References and Notes

- (1) Maciejewski, A.; Steer, R. P. *Chem. Rev.* **1993**, 93, 67.
- (2) Ramamurthy, V.; Steer, R. P. *Acc. Chem. Res.* **1988**, 21, 380.
- (3) Maciejewski, A.; Demmer, D. R.; James, D. R.; Safarzadeh-Amari, A.; Verrall, R. E.; Steer, R. P. *J. Am. Chem. Soc.* **1985**, 107, 2831.
- (4) Burdzinski, G.; Kubicki, J.; Maciejewski, A.; Steer, R. P.; Velate, S.; Yeow, E. *Molecular and Supramolecular Photochemistry*; Ramamurthy, V., Schanze, K. S., Eds.; Marcel Dekker: New York, Submitted for publication.
- (5) Tittelbach-Helmrich, D.; Steer, R. P. *Chem. Phys. Lett.* **1996**, 262, 369 and references therein.
- (6) Ho, C. J.; Motyka, A. L.; Topp, M. R. *Chem. Phys. Lett.* **1989**, 158, 51.
- (7) Maciejewski, A. *J. Photochem. Photobiol. A* **1990**, 50, 87.
- (8) Lorenc, M.; Maciejewski, A.; Ziolk, M.; Naskrecki, R.; Karolczak, J.; Kubicki, J.; Ciesielska, B. *Chem. Phys. Lett.* **2001**, 346, 224.
- (9) Kubicki, J.; Maciejewski, A.; Milewski, M.; Wrozowa, T.; Steer, R. P. *Phys. Chem. Chem. Phys.* **2002**, 4, 173.
- (10) Burdzinski, G.; Maciejewski, A.; Buntinx, G.; Poizat, O.; Toeke, P.; Zhang, H.; Glasbeek, M. *Chem. Phys. Lett.* **2004**, 393, 102.
- (11) Proposito, P.; Marks, D.; Zhang, H.; Glasbeek, M. *J. Phys. Chem. A* **1998**, 102, 8894.
- (12) Toeke, P.; Zhang, H.; Glasbeek, M. *J. Phys. Chem. A* **2002**, 106, 3651.
- (13) Maciejewski, A.; Naskrecki, R.; Lorenc, M.; Ziolk, M.; Karolczak, J.; Kubicki, J.; Matysiak, M.; Szymanski, M. *J. Mol. Struct.* **2000**, 555, 1.
- (14) Nakayama, T.; Amijima, Y.; Ibuki, K.; Hamanoue, K. *Rev. Sci. Instrum.* **1997**, 68, 4364.
- (15) Lorenc, M.; Ziolk, M.; Naskrecki, R.; Karolczak, J.; Kubicki, J.; Maciejewski, A. *Appl. Phys. B* **2002**, 74, 19.
- (16) Ziolk, M.; Lorenc, M.; Naskrecki, R. *Appl. Phys. B* **2001**, 72, 843.
- (17) Szymanski, M.; Maciejewski, A.; Kozlowski, J.; Koput, J. *J. Phys. Chem. A* **1998**, 102, 677.
- (18) Bhattacharyya, K.; Das, P. K.; Ramamurthy, V.; Pushkara Rao, V. *J. Chem. Soc., Faraday Trans. 2* **1986**, 82, 135.
- (19) Burdzinski, G.; Buntinx, G.; Poizat, O.; Lapouge, C. In preparation.
- (20) Akimoto, S.; Yamazaki, I.; Sakawa, T.; Mimuro, M. *J. Phys. Chem. A* **2002**, 106, 2237.
- (21) Burdzinski, G.; Maciejewski, A.; Buntinx, G.; Poizat, O.; Lefumeux, C. *Chem. Phys. Lett.* **2003**, 368, 745.
- (22) El-Sayed, M. A. *J. Chem. Phys.* **1962**, 36, 573.
- (23) El-Sayed, M. A. *J. Chem. Phys.* **1963**, 38, 2834.